AD-A179 607 ON THE BREAKDOWN OF THE WAVE PACKET TRAILING A TURBULENT SPOT IN A LAMINAR LAYER(U) TEL-AVIV UNIV (ISRAEL) A GLEZER ET AL. JAN 86 AE-85-2 1/1

UNCLASSIFIED AFOSR-TR-87-0388 AFOSR-84-0333 F/G 20/4 NL

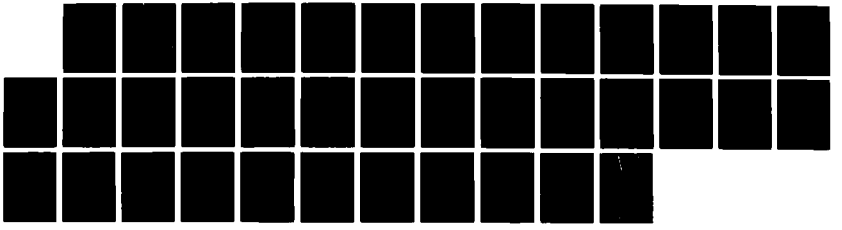

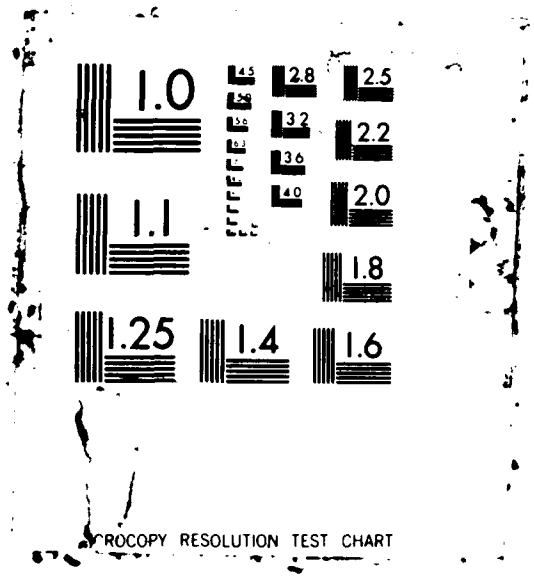
1.0
1.1
1.25
1.4
1.6
2.8
3.2
3.6
4.0
2.5
2.2
2.0
1.8
ROCOPY RESOLUTION TEST CHART

UNCLASSIFIED

SECURITY CLASSIFICATION OF THIS PAGE (When Data Entered)

REPORT DOCUMENTATION PAGE

READ INSTRUCTIONS BEFORE COMPLETING FORM

1 REPORT NUMBER: AFOSR-TR- 87-0388

2 GOVT ACCESSION NO.

3 RECIPIENT'S CATALOG NUMBER

4 TITLE (and Subtitle)

ON THE BREAKDOWN OF THE WAVE PACKET TRAILING A TURBULENT SPOT IN A LAMINAR BOUNDARY LAYER

5 TYPE OF REPORT & PERIOD COVERED

INTERIM FY 84-85

6 PERFORMING ORG. REPORT NUMBER

AE 85-2

7 AUTHOR(s)

A. Glezer, Y. Katz and I. Wygnanski

8 CONTRACT OR GRANT NUMBER(s)

AFOSR-84-0333

9 PERFORMING ORGANIZATION NAME AND ADDRESS

Tel-Aviv University
Ramat-Aviv, Tel-Aviv, 69978, Israel

10 PROGRAM ELEMENT, PROJECT, TASK AREA & WORK UNIT NUMBERS

61102F/2307/A2

11 CONTROLLING OFFICE NAME AND ADDRESS

Air Force Office of Scientific Research
Building 410, Bolling AFB D C 20332-6448

12 REPORT DATE

Jan 86

13 NUMBER OF PAGES

41

14 MONITORING AGENCY NAME & ADDRESS (if different from Controlling Office)

EOARD
223/231 Old Marylebone Road,
London NW1, UNITED KINGDOM

15 SECURITY CLASS. (of this report)

UNCLASSIFIED

15a DECLASSIFICATION/DOWNGRADING SCHEDULE

16 DISTRIBUTION STATEMENT (of this Report)

17 DISTRIBUTION STATEMENT (of the abstract entered in Block 20, if different from Report)

18 SUPPLEMENTARY NOTES

19 KEY WORDS (Continue on reverse side if necessary and identify by block number)

Boundary layer, Tramsition, Stability, Hot wire anemometry

20 ABSTRACT (Continue on reverse side if necessary and identify by block number)

The evolution of two oblique wave packets trailing the transitional spot was investigated in order to determine the extent of the interaction between the packets and the spot. The experimental investigation, carried out in two slightly different laminar boundary layers characterized by Falkner-Skan parameters of 0 and 0.2, revealed the importance of miniscule pressure gradients on the stability of the laminar boundary layer and the rate at which it can be contaminated by a turbulent spot. Some simple, novel statistical procedures for treating the data were developed and were used to accentuate the understanding of the physical processes governing transition to turbulence.

DD FORM 1 JAN 73 1473 EDITION OF 1 NOV 65 IS OBSOLETE

UNCLASSIFIED

SECURITY CLASSIFICATION OF THIS PAGE (When Data Entered)

ON THE BREAKDOWN OF THE WAVE PACKET TRAILING A TURBULENT SPOT IN A LAMINAR BOUNDARY LAYER

A. Glezer, Y. Katz, and I. Wygnanski

January 1986

ABSTRACT

The evolution of two oblique wave packets trailing the transitional spot was investigated in order to determine the extent of the interaction between the packets and the spot. The experimental investigation, carried out in two slightly different laminar boundary layers characterized by Falkner-Skan parameters of 0 and 0.2, revealed the importance of miniscule pressure gradients on the stability of the laminar boundary layer and the rate at which it can be contaminated by a turbulent spot. Some simple, novel statistical procedures for treating the data were developed and were used to accentuate the understanding of the physical processes governing transition to turbulence.

1. INTRODUCTION

The appearance of turbulent spots in a laminar boundary layer marks the final stages of the transition process because the turbulence contained in these spots spreads in all directions, contaminating the laminar flow. The mechanism by which the spots entrain vortical fluid from within the boundary layer and irrotational fluid from above is still not understood, in spite of the numerous investigations carried out recently. The purpose of this investigation is to shed some light on the manner in which the spot destabilizes the surrounding laminar boundary layer and enables turbulent interfaces to propagate into the nonturbulent fluid in both lateral and longitudinal directions.

The instability of the laminar boundary layer to small, random disturbances is well known. Amplification rates of plane Tollmien-Schlichting waves were verified experimentally by Schubauer and Skramstad (1948), and the evolution of a small-amplitude wave packet was examined theoretically by Gaster (1975) and experimentally by Gaster and Grant (1975). The nonlinear

aspects of the phenomenon leading to rapid amplification and the eventual breakdown to turbulence remain an enigma to date. Klebanoff et al. (1962), as well as Kovasznay et al. (1962), managed to localize the breakdown of Tollmien-Schlichting waves by adding spanwise irregularities to the flow, which resulted in the creation of streamwise vortices downstream of those irregularities and a concomitant establishment of an inflexional velocity profile. The velocity profile created in this manner is inviscidly unstable to small disturbances, leading to rapid amplification and the generation of turbulence. Kovasznay et al. mapped the vorticity contours associated with the initial breakdown to turbulence. In plan view, the shape of these contours resembles the boundaries of a turbulent spot.

Natural transition to turbulence occurs at discrete locations which are presumably associated with undetectably small irregularities in the experimental apparatus. It is well known that the concentration of oscillating vorticity, at locations corresponding to the onset of turbulence, stems from the very rapid amplification which occurs prior to breakdown. Turbulent spots are generated so swiftly that their evolution from an instability is only vaguely described in the literature. There are speculations suggesting that the evolution of shear waves may be entirely bypassed by some unknown, presumably inviscid, yet explosively amplified instability (Morkovin 1969).

The renewed interest in turbulent spots stems in part from the need to chart quantitatively the large coherent eddies in a fully developed turbulent boundary layer. This task still presents a major challenge to researchers in the field who, thus far, have only been able to provide some descriptive information. It has been demonstrated (Zilberman et al. 1976) that some portions of the spot retain their identity in a fully developed turbulent boundary layer over extremely long distances. The identifiable portions of the

spot exhibit features in detailed agreement with the observed characteristics associated with the large coherent eddies; the two may therefore be identical. Flow visualization (Cantwell et al. 1978, Perry et al. 1981) indicates that the large eddies situated in the interior of a turbulent spot are not different from the eddies existing in turbulent boundary layers. The eddies located near the boundaries of the spot, particularly at its spanwise extremities, might be the most recent large structures added to the spot and may therefore be more clearly identifiable experimentally. Furthermore, these eddies may be the product of the destabilization of the laminar boundary layer and perhaps may be correlated with a classical (presumably nonlinear) stability analysis.

An isolated spot, in the absence of pressure gradient, is often trailed by two oblique wave packets whose frequency, wave speed, and amplitude distribution across the boundary layer correspond to the Tollmien-Schlichting waves which had undergone the largest amplification (Wygnanski et al. 1979). The waves attain their maximum amplitude behind the "wing tips" of the spot, yet no waves were ever observed near the plane of symmetry. Since the group velocity of the wave packet is inclined to the plane of symmetry at an angle which is identical to the spreading angle of the spot itself, one can conclude that the two are correlated and that these waves are an important element in the transition process. This conclusion was reinforced by the observation that, at high Reynolds numbers, some of the waves in the packet break down and generate new spots, thus setting up a chain reaction by which turbulence spreads in the boundary layer. The interplay between a single spot and its trailing wave packet is further complicated by the fact that, at moderate Reynolds numbers, the distance separating the two increases with time while the spot travels downstream and keeps spreading in the spanwise and streamwise directions.

Gad-El-Hak et al. (1981) estimated that the rate of growth of the spot in the lateral direction is an order of magnitude larger than its rate of growth normal to the solid surface. They argued that the turbulent region is surrounded by irrotational fluid only in the direction normal to the surface and that the entrainment through this interface is governed by viscous forces, as observed by Corrsin and Kistler (1955). In the lateral and longitudinal directions, the spot is surrounded by vortical fluid which can be destabilized by disturbances induced by the spot. The destabilization of the laminar boundary layer is much more vigorous than the entrainment of irrotational fluid. Gad-El-Hak et al. verified these conjectures by flow visualization. They marked the initial patch of turbulence with dye and observed that the dye did not diffuse laterally, as did the boundaries of the spot. The tagged turbulent fluid mixed rather slowly with the surrounding fluid, even when the latter was also turbulent. Their hypothesis of destabilization does not correlate with the classical stability analysis because the wave lengths which they observed were much shorter than predicted, while the amplification rates were faster than expected theoretically. Chambers and Thomas (1983) attempted to establish the relationship between the spot and the wave packet trailing it by flow visualization at a fairly low Reynolds number. They did not observe any breakdown of the wave packets into turbulence, therefore questioning the universality of the earlier observations by Wygnanski et al. (1979). They suggested that the wave packets are merely passive attendants to the spot.

This manuscript describes some experiments linking the wave packet to the growth of the spot. It is a step in a continuing effort aimed at improving our understanding of the transition process and possibly exerting some measure of control over it. The measurements were made in the low-speed wind tunnel facility at Tel-Aviv University at a free stream velocity of 11.4 m/s, corresponding to Reynolds numbers based on the displacement thickness of the

laminar boundary ranging from 1000 to 1500.

2. EXPERIMENTAL APPARATUS AND DATA REDUCTION

The basic experimental appartus is not new. The facility and the ancillary equipment used in this experiment are described in the archival literature in conjunction with earlier work (e.g., Wygnanski et al. 1975). The spot was generated by a spark, approximately 2 mm in length, discharging in the spanwise direction near the surface of the plate and located 300 mm from its leading edge. The streamwise velocity component was measured with a rake of 10 hot wires spanning the height of the laminar boundary. Five hundred events, having a duration of 128 msec each, were recorded at every point. Measurements were taken at numerous streamwise stations at intervals of 5 mm in the spanwise direction extending beyond the wing-tip of the spot. The hot-wire rake, while butting the surface, positioned the nearest wire approximately 0.5 mm above the plate; the nominal distance separating adjacent pairs of the first six of the wires in the rake was also 0.5 mm (providing six data points in 3 mm). The data were ensemble-averaged, and curves were fitted to all the velocity profiles measured at each instant in time. This procedure yields a composite velocity field at any given (X, Y) coordinate as a function of the span, Z, and the time, T.

Measurable pressure gradients on the surface of the plate were removed by adjusting the angle of attack of the plate and the top and bottom walls of the wind tunnel while monitoring the surface pressure. Residual gradients were completely eliminated by making fine adjustments to tunnel walls while monitoring the velocity profile until it fitted best the theoretical profile predicted by Blassius (i.e., Falkner-Skan constant $\beta = 0$). Minute pressure gradients, immeasurable by conventional means, easily affected the shape of the velocity profile, changing the value of β from 0 to 0.2.

The turbulent intensity of the streamwise velocity component, defined in the classical manner

$$\overline{u'^2} = \lim_{T\to\infty} \frac{1}{T} \int_0^T (U - \bar{U})^2 \, dt \tag{2.1}$$

(where U is the instantaneous velocity, $\bar{U}$ is the mean velocity, and T is the time of integration), can be extended to a nonstationary process (e.g., Van Atta and Helland 1980; see also Antonia et al. 1981),

$$\langle \overline{u'^2} \rangle_j = \frac{1}{N} \sum_{I=1}^{N} [U(I, J) - \langle U(I,J) \rangle]^2 \tag{2.2}$$

where $\langle U(I,J) \rangle$ represents an ensemble-averaged velocity and N is the number of realizations used in obtaining the average.

In order to avoid errors arising from averaging over spots of different sizes, shapes, and celerities, a different scheme for calculating the intensity of turbulent fluctuations was devised by replacing $\langle U(I,J) \rangle$ with $\hat{U}(I,J)$, a pseudo "mean" velocity of <u>each</u> realization. This "mean" may be thought of as the line that an experienced person would draw on the plot of a velocity trace resulting from the passage of an individual spot. Since the data are not stationary, a simple filter may not provide this result.

$\hat{U}(I, J)$ was computed by a running-average technique with a variable time window. This is a double-pass scheme. A time window is selected in the first pass and is centered on successive data points. The mean time derivative of the velocity data within the window is computed for each center point. In the second pass, the width of the original window at each data point is varied

proportionately to the time derivatives computed in the first pass, and the center point is replaced by the mean of the other data points included in the new window. The maximum width of the window in the turbulent zone encompassed 17 points, corresponding to 8 msec, while no averaging was necessary in the laminar boundary layer.

The presence of turbulence in the core of the spot is indicated by intermittency, ideally defined in terms of oscillating vorticity and therefore small-scale fluctuations. The intermittency in the present experiment was determined digitally from the streamwise component of velocity (Glezer and Coles 1986). Given a uniformly spaced time series U(I), consider a least squares fit of a straight line to three successive data points. The fitted line is parallel to a line passing through the first and third points but is displaced from it by a distance B. The R.M.S. deviation of the three points from the line is

$$\epsilon = \sqrt{2}\, B \tag{2.3}$$

where

$$B = \frac{1}{2}\left[U_i - \frac{1}{3}\left(U_{i-1} + U_i + U_{i+1}\right)\right]$$

Whenever ϵ exceeds a prescribed threshold level, the flow is assumed to be turbulent.

An effort was made to reduce the ambiguity in the mean quantities due to jitter in the arrival time and the duration of the spot. A simple ensemble-averaged velocity, conditionally triggered by the signal generator which also initiated the spot, was calculated first. Each event was correlated with the ensemble average and shifted in time until the deviation from the ensemble was minimized. The time shifts for each realization were recorded and used for averaging of all other quantities considered.

3. DISCUSSION OF RESULTS

3.1 Experiment at $\beta = 0$

The first objective of this investigation was to reconcile the differences between the observations of Chambers and Thomas (1983) and the earlier observations of Wygnanski et al. (1979). The goal was therefore to establish the conditions leading to the breakdown of the waves following the spot and to determine whether the turbulence resulting from such a breakdown contributes to the growth of the spot.

Contours of average velocity perturbation $(U - U_{LAM})/U_1$ resulting from the passage of the spot are shown in Figure 1. These data were plotted in the Z-T plane 1 mm above the surface (at $y/\delta^* = 0.6$). The contour levels vary between +1% and +10% at intervals of 1% relative to the undisturbed laminar velocity profile and between -0.5% and -2.5% at intervals of -0.5%. These measurements were taken at X = 92, 110, and 130 cm downstream of the leading edge, corresponding to X_s = 620, 810, and 1000 mm from the spark. The leading edge of the spot and, in particular, its tip are easily recognizable by the steep gradients in the velocity perturbation levels. One may therefore choose either the 2% perturbation level (Coles and Barker 1975) or even the 10% level to mark the average location of the leading interface of the spot with reasonable accuracy. The trailing interface of the spot cannot be detected on these contour maps because, at this elevation above the surface, the "calmed region" (in the parlance of Schubauer and Klebanoff 1956) perturbs the laminar profile in a fashion similar to turbulence. The 10% perturbation contour outlining the edge of the calmed region at X_s = 1000 mm bulges outward from the spot when compared to similar contours plotted for smaller values of X. The wave packet is clearly visible on these plots (which is the reason for

choosing this particular elevation in the first place). The waves attain their maximum amplitude at $Z/X_s = 0.12$, and they decay or blend with the calmed region at smaller values of Z/X. The amplitude and span of the waves diminish beyond $X_s > 900$ mm for reasons which will be discussed later. The spot induces a region of low velocity near the surface of the plate and beyond its tip by presumably lifting some low-speed fluid from the surface upwards. The waves appear to originate in the tip region, suggesting that it may be more unstable to small disturbances than most of the surrounding laminar boundary layer. This region moves with the tip of the spot while the velocity of the waves is generally slower and, hence, the distance between the waves and the spot increases with time. The spot also induces an upwash along its entire leading edge (Wygnanski et al. 1982), but this upwash is more confined to the immediate neighborhood of the interface and therefore, perhaps, waves were seldom visible in this region. It is clear that the breakdown of the waves cannot be determined from ensemble-averaged mean velocity data, although the distorted contours at $X_s = 1000$ mm may be indicative of this process.

The presence of an interface separating turbulent from nonturbulent fluid outside the main body of the spot could, in principle, serve as a measure for the breakdown of the waves (Figure 2). This interface is traditionally determined by a frequency-filtering operation forming an envelope to any rapidly fluctuating quantity and replacing this envelope by a telegraph signal. Such a procedure is not entirely objective as it requires an arbitrary determination of the threshold level which triggers the telegraph signal. At a given location, some or all of the waves associated with a single event may or may not break down. Furthermore, when breakdown occurs, the duration of the turbulent region, its intensity, and the time of its appearance vary considerably from one realization to the next. As a result, the mapping of the new turbulent interface becomes somewhat dubious, and the largest values

of the intermittency factor (i.e., the ensemble-averaged telegraph signal) in a wave packet undergoing transition is a fraction which may never approach unity. The corresponding value of $\gamma = 0.5$, which signifies the average shape and size of the spot, no longer signifies the average location of the turbulent interface marking the boundaries of the wave packet. Nevertheless, the determination of γ is useful because it indicates the presence or absence of turbulence. The contours of intermittency shown in Figure 5a (below) indicate quite clearly that a turbulent region appears behind the spot at X_s=810 mm, grows in size, and partially amalgamates with the parent spot at X_s=1000 mm.

A physically meaningful definition of turbulent intensity is more informative than intermittency in attempting to understand the transition to turbulence of the wave packet and the destabilization process of the laminar boundary layer by the spot. The conventionally defined turbulent intensity [equation (2.1)] is prone to errors arising from a jitter in the time of arrival of the spots and a variance in their length, breadth, and shape at any streamwise location. All these quantities contribute to the difference between the ensemble-averaged velocity and the instantaneous velocity, creating an apparent turbulent intensity near the leading and trailing interfaces of the spot. When this apparent intensity is averaged over many realizations, it smooths (or smears) the actual gradients existing near the interface of the spot. An example of the errors that might occur in this procedure is shown in Figure 3, in which the solid line represents the ensemble-averaged perturbation velocity and the dotted line superposed on it represents the same perturbation velocity trace produced by a single realization; most of the fluctuating intensity plotted below is, of course, erroneous. In order to avoid these errors, a new scheme, described in section 2, for calculating the intensity of the turbulent fluctuations was devised.

The validity of the new scheme is demonstrated in Figure 4, where representative temporal records of the streamwise velocity component, taken at various stages of wave breakdown, are shown. The thin line, visible only when the flow was turbulent, represents the measured velocity and the "+" symbols correspond to the pseudo "mean" (see section 2) associated with these specific realizations. The waves depicted in Figure 4a are not broken; they have a large amplitude comparable to the perturbation velocity produced by the spot. The waves shown in Figure 4b just started to break down, while those shown in Figure 5c degenerated into a patch of turbulence. It is quite clear that the procedure described in section 2 distinguishes between the low-frequency oscillations associated with the passage of the spot or the waves and the high frequencies signifying turbulence, yet it does not contribute to an erroneous turbulent intensity resulting from a phase or amplitude mismatch between the ensemble and the individual realizations.

Three contour maps of the ensemble-averaged turbulent intensity (u'/U_1) plotted in the (Y, T) plane for $Z/X = 0.08$ are shown in Figure 6. These contours provide additional evidence for the transition to turbulence occurring in the wave packet. At $X_s = 620$ mm, no breakdown was observed since all intensity contours reside within a well-defined single structure. Farther downstream, the distribution of turbulent intensity is disfigured by a second turbulent region following the spot. At $X_s = 810$ mm, the intensity of the turbulence trailing the original spot is only one-half of the intensity of turbulence within the spot but, at $X_s = 1000$ mm, this ratio is larger. The difference in the intensity levels inside the secondary turbulent region is, in part, a reflection of the fraction of wave packets that break down at every location. The distribution of turbulent intensity within the spot changes with X as well. For example, the highest average turbulent intensity ($u'/U_1 > 10\%$) measured at $X_s = 620$ mm occurs at a time corresponding to the passage of the

ridge (or apex) of the spot at this (X, Z) coordinate but, at X_s = 810 mm and even more so at X_s = 1000 mm where the spot is much larger, the region of highest turbulent intensity (which is down to 7%) has shifted toward the leading interface (Figure 6).

Contour plots of the turbulent intensity in the (Z, T) plane are shown in Figure 5b. The average boundaries of the spot, defined by the locus of points at which $\gamma = 0.5$, are also marked on this figure. The gradual decrease in the turbulent intensity near the boundaries of the spot stems from averaging the data over spots of different dimensions and shapes; it does not represent a true gradient in the turbulent intensity within the spot. The high turbulent intensity observed near the wing tip of the spot and near its leading edge at all values of X can only be explained by an enhanced turbulence production in this region. The observations made in the (Y, T) plane (Figure 6) also indicate that the highest turbulent intensities occur near the leading interface of the spot where the average $\gamma \ll 1$. Thus, an averaging procedure that will take into account the differences among individual realizations is required. A representative turbulent intensity distribution within an ensemble-averaged spot may be obtained by dividing the measured intensity by the local intermittency factor γ, yielding the equivalent of corrected zone-averaged data for nonstationary flows (Figure 5c). Since the present procedure of detecting turbulent intensity eliminated all fluctuations existing outside the turbulent zone, the division by γ gives the correct turbulent zone average, provided one does not carry the procedure to its limit (i.e., $\gamma \to 0$). In the contour plots shown in Figure 5c, the calculation procedure was stopped whenever $u'/U < 2\%$. Setting the cutoff at different threshold levels either in γ or in u'/U did not alter the qualitative behavior of the corrected turbulent intensity contours. These contours not only reveal the existence of much sharper gradients near the boundaries of the spot, but also the existence of much higher levels of

turbulent intensities near the boundaries. Although the precise ratio between the intensity of the turbulence near the boundary to the turbulent intensity in the center of the spot depends to some extent on the method and the threshold levels used in computing the intermittency data, a variety of cross-checks verified the general validity of the results.

The corrected turbulent intensity contours indicate an enhanced activity near the leading interface of the spot, where the average level is approximately twice as high as it is in the core of the spot. The highest corrected turbulence level recorded occurs in the juncture between the parent spot and the turbulent patch at X_s = 810 mm and farther downstream. This location probably coincides with the crest of a wave that broke down first. As the turbulent patch increases, the turbulence level at its center decreases and the boundary separating the parent spot from the patch is moved outward toward the tip of the parent spot. The highest level of corrected turbulent intensity at X_s = 620 mm (i.e., where the wave packet does not yet undergo transition to turbulence) occurs in the tip areas. The fact that the ensemble-averaged and the corrected turbulent intensities are much lower near the center of the spot than near its boundaries suggests that turbulence is generated along the peripheries of the spot. At this elevation from the surface, which is under the "overhang" (i.e., the most forwardly protruding turbulent region in the leading interfaces of the spot), fluid is vigorously entrained by the leading interface (Wygnanski et al. 1979) or, conversely, the laminar boundary layer in this region is highly destabilized by the approach of the leading edge of the spot which may be viewed as a large vortex. The level of turbulent intensity in many flows undergoing transition is usually well above the level prevailing in fully developed turbulent flows (e.g., the turbulence level near the interface of a slug in transitional pipe flow; Wygnanski and Champagne 1973), thus the peripheral area of the spot is no

exception. This suggests that the leading edges of the patch and the parent spot are very active in destabilizing the surrounding laminar boundary layer, in spite of the fact that entrainment considerations near the plane of symmetry suggest that most of the turbulent activity occurs at the trailing interface. Gad-El-Hak et al. (1981) also observed a strong destabilization of the laminar boundary layer under the overhang of the leading interface.

Kovasznay et al. (1962) observed that the initial breakdown to turbulence in a boundary layer excited by a vibrating ribbon occurs at the outer part of the laminar boundary layer coinciding with the location of the "overhang." For this reason, the turbulent intensity contours are plotted at this elevation (Figure 7). The results indicate that the turbulent activity near the leading interface ceased, while the turbulent intensity near the tip of the parent spot and the turbulent patch increased by at least 50%. This suggests that the spot grows in the spanwise direction by amplifying the waves originating from the low-velocity region induced by the tip and in the streamwise direction by amplifying perturbations beneath the overhang.

The corrected turbulent intensity contours at the spanwise edge of the turbulent patch are wavy, in spite of the fact that neither the intermittency contours nor the ensemble-averaged intensity contours exhibit such behavior. The wavy pattern results from the manner in which the contours of turbulent intensity and intermittency cross one another. This will occur whenever a wave starts to break at some location along the crest (usually at a location at which the wave crest attained its highest amplitude) and the breakdown process progresses along the wave crest. This is analogous to the formation of surf in shallow-water waves. The intensity of turbulence at the location that first broke down increases with time, while the turbulent fluid is convected with the crest of the wave. The boundary at which turbulence is

first observed (as identified by the telegraph signal) moves, therefore, along the wave crest and away from the region in which turbulence intensifies, resulting in a very sharp angle marking the intersection between the contours of turbulent intensity and the border of the turbulent region. When the results are ensemble-averaged, the latter curve is replaced by intermittency contours. The wavy contours at the extremities of the turbulent patch (whose characteristic time scales coincide with the periods of the observed waves) and the associated high levels of the corrected turbulent intensity (Figures 5c and 7) reflect the history of transition to turbulence within the wave packet. One may speculate that this is also the mechanism by which the spot destabilizes the boundary layer in the transverse direction, because the corrected turbulent intensity near the tip of the spot exhibits characteristics similar to those of the wave packet that disintegrated into a turbulent patch. The direct degeneration of the wave crests into turbulence was not observed in this region, perhaps because of the speed at which this process takes place in the present experiment.

It was shown (Figures 5-7) that for $X_s > 620$ mm (corresponding to $Re^*_\delta = 1140$), some wave crests in the packet become turbulent, generating a new region which increases in size as it proceeds downstream. Since the laminar wave packet lags behind the spot, a separate turbulent patch in the shape of a small spot emerges upon breakdown just upstream of the wing tip of the parent spot (see also Wygnanski et al. 1979). However, in time, the leading edge of this turbulent patch accelerates, catching up with the trailing edge of the parent spot and slowly amalgamating with it.

One may attribute the change in the shape of the plan view of the spot with time or with increasing downstream distance to the amalgamation process occurring between the turbulent patch and the parent spot. In fact, a small spot is initially triangular in shape, having a straight trailing edge

perpendicular to the direction of streaming (Matsui 1980, Gad-El-Hak et al. 1981, Chambers and Thomas 1983), while a large and mature spot has a more concave trailing interface resembling an arrowhead shape (Cantwell et al. 1978). The corrected turbulent intensity contours which extend all the way to the plane of symmetry of the spot (Figure 7c) indicate that the "calmed region" is not affected initially by the new turbulent patch. The corrected turbulent intensity in the patch (Figure 7c) increases almost monotonically with increasing Z, indicating that the waves may keep breaking down at large Z while the "oldest" turbulence in the patch resides near the plane of symmetry. When the experiment is carried out at much higher free stream velocity (Wygnanski et al. 1979), the turbulent patch retains its separate entity over larger streamwise distances, which may be attributed in part to more rapid convection of the spot.

3.2 Experiments at $\beta = 0.2$

The boundary layer in the experimental observations discussed above was marginally stable to small disturbances for $X_s < 350$ mm (corresponding to $Re^*_\delta = 500$). This resulted in an initial decay of the waves. Farther downstream, the boundary layer became unstable, causing amplification and eventual breakdown of the waves. Since the stability of the boundary layer to small disturbances is greatly affected by the pressure gradient (Wazzan et al. 1968), the same may hold for the amplification of the wave packet accompanying the spot. Some aspects of the experiment were therefore repeated in the presence of a slightly favorable pressure gradient for the purpose of delaying the breakdown process. The mean velocity profile was described by a Falkner-Skan parameter, $0.1 < \beta < 0.2$, which was also reported in the investigation by Cantwell et al. (1978). The pressure gradient required to produce this

deviation from the Blassius velocity profile was immeasurably small, yet the critical Reynolds number increased from 500 at $\beta = 0$ to 2800 at $\beta = 0.2$.

The average velocity perturbations resulting from the passage of the spot at $X_s = 620$ mm were compared for both values of β. The two spots are qualitatively similar, although the overall dimension of the spot corresponding to $\beta = 0.2$ and the amplitude of the waves following it were somewhat diminished by the favorable pressure gradient. The turbulent intensity calculated farther downstream did not exhibit any breakdown of waves so clearly visible in Figures 5 and 6. Hence, these conditions were deemed suitable for a study of the behavior of the wave packet, the establishment of its origin, and its possible link with the selective destabilization of the boundary layer in the vicinity of the spot.

A typical ensemble-averaged velocity record obtained beyond the wing tip of the spot at $X_s = 580$ mm, $y = 1$ mm, and $Z = 90$ mm (Figure 8) clearly shows the region of low velocity induced by the spot, which serves as a moving generator for the wave packet emanating from it. The velocity perturbation induced by the spot's wing tip resembles the velocity field associated with a Rankine vector. It is easy to analyze the characteristic parameters of the wave packet from the ensemble-averaged records, provided the average data are not obliterated by the averaging process. Spectral analysis of the averaged data indicates that the predominant frequency of the waves in the packet varies between 80 and 100 Hz. In order to establish the relevance of these findings, a similar analysis was applied to the individual realizations. The signals were low-pass filtered and hanned (see also Wygnanski et al. 1979), and the ensemble-averaged frequency of the waves was again in the range of 80 to 100 Hz. A schematic representation of the averaged wave packet in a coordinate system moving with the spot is shown in Figure 9 for $600 < X_s <$

720. The boundaries of the spot are represented in this figure by turbulent intensity contouring varying from 5% to 6%; the size of the tick-marks represents the local amplitude of the wave crest of the ensemble-averaged velocity signal. The waves extend in the spanwise direction beyond the boundaries of the spot, but they do not appear in the calmed region trailing the spot. At X_s = 600 mm, only three wave crests are visible in the packet, but, at X_s = 680 mm, a new wave crest emerged from the low velocity region induced by the spot, increasing the number of crests in the packet to four. The maximum amplitude of wave "1" in the packet is approximately doubled between X_s = 580 and X_s = 740 mm. The maximum amplitude of this wave crest propagates along the ray Z/X_s = 0.14 which forms an angle of 8` with the plane of symmetry of the spot. The maximum amplitude of the second crest does not change with $X_s$ over the range considered; it propagates along a ray defined by $Z/X_s$ = 0.125, therefore diverging from the plane of symmetry at a smaller angle of 7`. The maximum amplitude of the third wave crest decays rapidly, while the corresponding maximum amplitude of the new wave crest increases with X.

In order to establish the relative position between the wave packet and the spot, the data acquired at X_s = 620 and X_s = 740 are superimposed on one figure. The coordinates chosen for this purpose are $U*t/X_s$ and Z/X_s because, in these coordinates, the boundaries of the spot remain invariant in the absence of breakdown (Figure 10). The "new wave" seen at X_s = 740 replaced the location of wave "1" seen at X_s = 620, while the gap between this wave crest and the trailing edge of the spot increased during the time of travel between these X locations. The average streamwise component of the propagation velocity of the wave crest is 0.32*U, while the trailing interface of the spot at this Y location is convected downstream at 0.5*U. The group

velocity of the wave packet was calculated after fitting an envelope to the ensemble-averaged, hanned, and filtered velocity data (Figure 11). The streamwise component of the group velocity measured between X_s = 600 mm and X_s = 720 mm at Z > 80 mm is 0.35*U, and it diminished to 0.3*U closer to the plane of symmetry. The waves in the packet are essentially nondispersive over the distance considered. Since the gap between the wave packet and the spot increases with X_s, the isolated packet probably does not contribute to the streamwise rate of growth of the spot in this range of Reynolds numbers at the favorable pressure gradient considered. This might have been the situation investigated by Chambers and Thomas (1983).

Closely spaced measurements of velocity perturbation in the laboratory coordinates enabled us to reconstruct the ensemble-averaged data in space at a given instant in time and therefore assess the true geometric relationship between the spot and the wave packet. The velocity perturbation in the XZ plane ($580 < X_s < 700$; $45 < Z < 110$) at times corresponding to 140 and 144 msec after the initiation of the spot are shown in Figure 12 without the customary stretching in the spanwise dimension. At large values of Z, the wave crests are inclined to the plane of symmetry at an angle of 45°. The wave crests turn toward the spot at smaller values of Z, and the resulting velocity perturbation associated with them should become more significant in the YZ plane. The streamwise streaks observed in the "calmed region" following the spot (Gad-El-Hak et al. 1981) may be associated either with the turning of the waves or with some remnants of longitudinal vortices present within the spot.

The change in the inclination angle of the averaged wave crests and the concomitant decrease in their amplitude raised the possibility that the averaging procedure might not have been physically meaningful. In order to

resolve this question, the characteristics of the wave packet seen at each realization were analyzed. The velocity signal was low-pass filtered at 200 Hz, and the time of occurrence of each wave trough was determined in addition to its amplitude relative to the surrounding crests. The results are shown in Figures 13a-d. (These measurements were taken at $X_s = 580$ and $50 < Z < 80$, i.e., between the first spanwise location at which waves have been observed and the spanwise location at which the amplitude of the waves, based on the ensemble-averaged velocity perturbation, is a maximum.) The ensemble-averaged velocity perturbation is also shown on each of the plots. At Z = 50 mm, waves were only observed in 20% of the events, and only in 12% of the occurrences was a clear wave crest surrounded by two troughs discerned. The time of occurrence of the troughs (Figure 13a) is not as repeatable as it is at larger values of Z. At Z = 80 mm, a wave packet was observed in approximately 75% of the occurrences: two wave troughs were seen in 30% of these events, three wave troughs occurred in 35%, and four troughs in approximately 10% of all the realizations. One may regroup the waves into numbers "1," "2," and "3" by considering a 10-msec time interval surrounding each peak in the histograms shown in Figure 13. For example, at Z = 80 mm, 288 events fall into the wave "1" category, 347 events into the wave "2" category, and 230 events into the wave "3" category. The average amplitude of these waves may be determined from this classification. One may also determine the average amplitude of waves "1" through "3" by considering only those wave packets in which three wave troughs have been observed (173 events out of a total of 500). The amplitudes of the wave troughs using either calculation scheme turned out to be almost identical, but they were quite different from the amplitudes calculated from the ensemble-averaged velocity records. The amplitudes of the waves, whenever they are discernible, increase monotonically with decreasing Z. If the amplitudes of these waves were to increase beyond a critical threshold

level, one would probably observe a breakdown of the type seen in the experiment conducted at $\beta = 0$. The waves seem to disappear in the vicinity of the "calmed region" because the number of realizations in which they are observed is greatly reduced. The "calmed region" in which the velocity profile is much more stable and more convex than it is in the unperturbed laminar boundary layer might be induced by the vortices within the spot, or it might be a product of interacting waves originating at both wing tips of the spot that amalgamated together while turning in the streamwise direction. The cause for the generation of the calmed region was never determined, and the hypothesis proposed here has yet to be proven. Nevertheless, whether the wave packet breaks down as a separate entity or disappears by generating the calmed region, it still remains part and parcel of the turbulent spot affecting, at least to some extent, the flow field in its vicinity.

The effects considered are intimately related to the local shape of the velocity profile and the rate of *divergence* of the laminar boundary layer in the direction of streaming because these two parameters govern the sensitivity of the boundary layer to extraneous disturbances over which one has limited control. The relationship between the growth of the spot, the breakdown of the wave packets, and the stability of the boundary layer may be further ascertained by solving the Orr-Sommerfeld equation for spatially growing disturbances, assuming that the velocity field produced by the passage of the spot describes the basic, given state of the flow. Contours of the dimensionless amplification rate for the predominant frequency of 95 Hz at U_1 = 11.4 m/s during the spot passage at X_s = 680 mm are shown in Figure 14. The boundaries of the spot at an elevation of 1 mm are also plotted for comparison. Although this calculation procedure may not be truly valid because

i. the perturbed flow field is three dimensional,

ii. the boundary layer diverges quite rapidly in some regions, and

iii. the possible interaction with turbulence was not considered,

the contours shown delineate clearly the unstable regions in this case. These regions coincide with the leading interface of the spot and with the "moving generator" located beyond its tip. The damped contours resemble the contours of the mean velocity perturbation and consequently the waves, after being amplified in the "moving generation," decay as they start lagging behind the spot. The detailed correspondence between these oversimplified calculations and the experiment are encouraging since they provide a tool for proper theoretical analysis.

3.3 Artificial Excitation of the Wave Packet

It was shown that a favorable pressure gradient decreases the rate of amplification of the wave packet thereby delaying the breakdown to turbulence. In order to confirm that the opposite argument holds true, one may either introduce an adverse pressure gradient into the flow or else retain the Blassius boundary layer ($\beta = 0$) and artificially enhance the amplitude of the wave packet trailing the spot. This was achieved by an external introduction of a disturbance which, by itself, evolves into a small-amplitude wave packet but otherwise favorably interacted with the packet trailing the spot, contributing to the increase of amplitudes of the waves within it and leading to an earlier breakdown. The latter possibility was explored because it offered new means of controlling the transition process and may reveal some aspects of the nonlinear nature of the interaction among waves. A disturbance was generated by a short pulse in the form of a momentary jet discharging at a right angle to the surface during the passage of the low-velocity region

induced by the wing tip of the spot. The jet emerged from a static pressure hole, 0.3 mm in diameter, located at X_s = 400 mm and Z = 80 mm and was generated by a small speaker attached to the underside of the plate. The cavity behind the static hole had to be filled with foam rubber so that the pressure fluctuations associated with the passage of the spot would not trigger a cavity resonance, which inadvertently always interacts with the wave packet. Thus, before proceeding with the experiment, it was verified that, in the absence of the external excitation, the spot and the waves trailing it were not affected by the presence or absence of the static hole.

The amplitude of the disturbance was adjusted in such a manner that it generated a weak wave packet, in agreement with the linear stability theory over the distances considered (see Gaster and Grant 1975). When the disturbance was introduced during the passage of the spot, the amplitude of the waves in the packet trailing the spot was increased, resulting in a premature transition to turbulence. Contours of turbulent intensity measured at three streamwise locations, X_s = 620, 700, and 780, at Z = 80 mm, with and without external excitation, are plotted in Figure 15 for the purpose of comparison. The size of the turbulent patch and the level of the turbulent intensity within it are greatly increased by the excitation at X_s = 620 and X_s = 700 (Figures 15a and 15b). The external excitation generated transition at β already at X_s = 620 mm which otherwise occurs naturally farther downstream. The effects of the momentary excitation fade away farther downstream (Figure 15c) because the duration, and therefore the spatial extent, at which the two packets interact is limited. This experiment proves that the amplitude of the waves trailing the spot affect the location of their transition which, in turn, influences the shape and the size of the spot.

4. CONCLUSIONS

Waves emerging from the low-velocity region outside the wing tip of the spot may amplify or decay, depending on the stability of the surrounding boundary layer. The wave packet may sometimes be a passive attendant to the turbulent spot or may sometimes be an active participant in the growth of the spot and the turbulent contamination of the laminar boundary layer. A turbulent patch generated by the breakdown of the waves increases in size while it propagates downstream, eventually amalgamating with the spot. The shape of the spot is therefore continuously changing with increasing distance from its generator because the trailing interface of the spot in a plan view becomes increasingly more concave with the passage of time. The front of the spot, acting as a large spanwise vortex, lifts off low-momentum fluid from the vicinity of the surface, actively destabilizing the boundary layer downstream of it. This destabilization, followed by transition, occurs so rapidly that the leading interface propagates downstream with a velocity commensurate to the maximum velocity of the flow.

REFERENCES

Antonia, R. A., Chambers, A. J., Sokolov, M., and Van Atta, C. W. 1981. J. Fluid Mech. 108, 317.

Cantwell, B., Coles, D., and Dimotakis, P. 1978. J. Fluid Mech. 87, 641.

Chambers, F. W. and Thomas, A. S. W. 1983. Phys. Fluids 26, 1160.

Coles, D. and Barker, S. J. 1975. Turbulent Mixing in Non Reacting and Reacting FLows (Murthy, ed.), Plenum Press.

Corrsin, S. and Kistler, A. L. 1955. Free Stream Boundaries of Turbulent Flows. N.A.C.A. Report 161244.

Gad-El-Hak, M., Blackwelder, R. F., and Riley, J. J. 1981. J. Fluid Mech. 110,

73.

Gaster, M. 1975. Proc. Roy. Soc. A. 347, 271.

Gaster, M. and Grant, I. 1975. Proc. Roy. Soc. A. 347, 253.

Klebanoff, P. S., Tidstrom, K. D., and Sargent, L. M. 1962. J. Fluid Mech. 12, 1.

Kovasznay, L. S. G., Komoda, H., and Vasudeva, B. R. 1962. "Detailed Flow Field in Transition." Proc. Heat Transfer and Fluid Mechanics Institute, Stanford Univ. Press, p. 1.

Matsui, T. 1980. Visualization of Turbulent Spots in the Boundary Layer Along a Flat Plate in a Water Flow" in Laminar-Turbulent Transition (R. Eppler and H. Fazel, eds.), Springer, p. 288.

Morkovin, M. V. 1969. Critical Evaluation of Transition From Laminar to Turbulent Shear Layers With Emphasis on Hypersonically Travelling Bodies." Flight Dynamic Lab. Report AFFDL-TR-68-149.

Perry, A. E., Lim, T. T., and Teh, E. W. 1981. J. Fluid Mech. 104, 387.

Schubauer, G. B. and Klebanoff, P. S. 1956. "Contributions on the Mechanics of Boundary Layer Transition." N.A.C.A. Report 1289.

Schubauer, G. B. and Skramstad, H. K. 1948. "Laminar Boundary Layer Oscillations on a Flat Plate." N.A.C.A. Report 909.

Van Atta, C. W. and Helland, K. N. 1980. J. Fluid Mech. 100, 243.

Wazzan, A. R., Okamura, T. T., and Smith, A. M. D. 1968. DAC 67086, Sept. 1, 1968, McDonnel Douglas Corp.

Wygnanski, I. J. and Champagne, F. H. 1973. J. Fluid Mech. 59, 281.

Wygnanski, I. J., Haritonidis, J. H., and Kaplan, R. E. 1979. J. Fluid Mech. 92, 505.

Wygnanski, I. J., Sokolov, M., and Friedman, D. 1975. J. Fluid Mech. 69, 283.

Wygnanski, I. J., Zilberman, M., and Haritonidis, J. H. 1982. J. Fluid Mech. 123, 69.

Zilberman, M., Wygnanski, I. J., and Kaplan, R. E. 1976. Phys. Fluids Suppl. 20, S258.

FIGURE CAPTIONS

1. Contours of velocity perturbation measured at $Y/\delta^* = 0.6$ and at X_s = 620 mm, 810 mm, and 1000 mm. The ordinate represents $50 \leq Z \leq 185$ mm and the abscissa, $0 \leq T \leq 128$ msec.
2. A typical 128-msec velocity record of the passage of the spot at X_s = 810 mm, Z = 85 mm, and $Y/\delta^* = 0.6$. Plotted below is a corresponding telegraph signal ($\varepsilon/U_1 = 0.4\%$; see eq. 2.3).
3. A comparison between a conventional rms signal (eq. 2.2) and a true rms signal (see caption for Fig. 2 for details).
4. A detection of wave-packet breakdown using the true rms procedure.
5. Contours of (a) intermittency, (b) rms, and (c) corrected rms as per notation in the caption of Figure 1.
6. Contours of true rms in the Y-T plane at $Z/X_s = 0.08$. The ordinate represents $0 \leq Y \leq 9$ mms and the abscissa, $0 \leq T \leq 128$ msec.
7. Contours of correlated rms in the Z-T plane at X_s = 620 mm, 810 mm, and 1000 mm at $Y/\delta^* = 1.75$, $0 \leq Z \leq 185$ mm.
8. An ensemble-averaged velocity perturbation beyond the wing tip of the spot.
9. The location of the wave crests relative to the spot. The size of the symbol represents the amplitude of the crest.
10. Superposition of the wave crests in dimensionless coordinates.
11. Determination of group velocity based on the envelope of the packet.
12. Contours of velocity perturbation in the X-Z plane at (1) T = 140 msec, (b) T = 142 msec, and (c) T = 144 msec. T is measured from the spark.
13. Histogram showing the number of troughs in the packet and their time of occurrence. The corresponding ensemble-averaged velocity perturbation is shown for reference.
14. Contours of spatial amplification (f = 96 Hz) based on data taken at X_s

= 680 mm for $\beta = 0.2$.

15. True rms contours in the T-T plane at (a) X_s = 620 mm, (b) 700 mm, and (c) 780 mm at Z = 85 mm. The contours on the right correspond to the excited flow.

X_s = 1000 mm

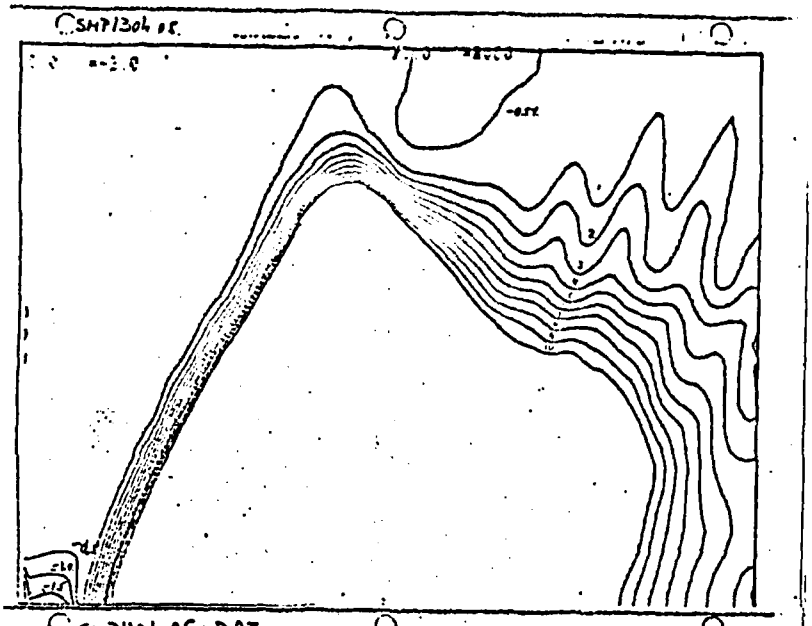

X_s = 810 mm

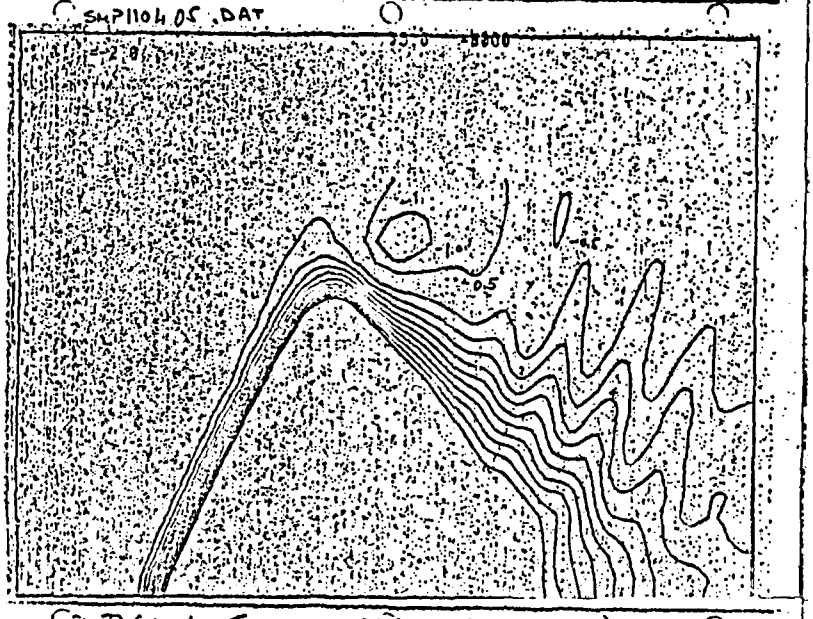

X_s = 620 mm

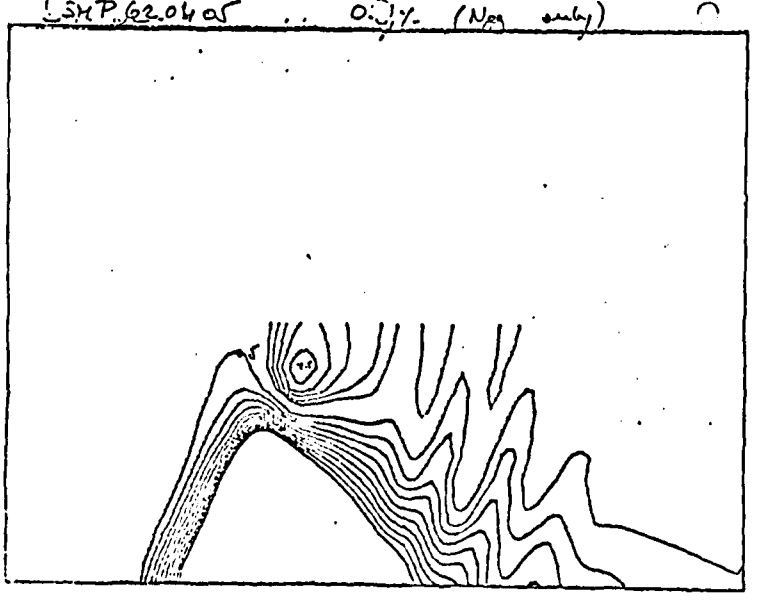

fig 1

(a)

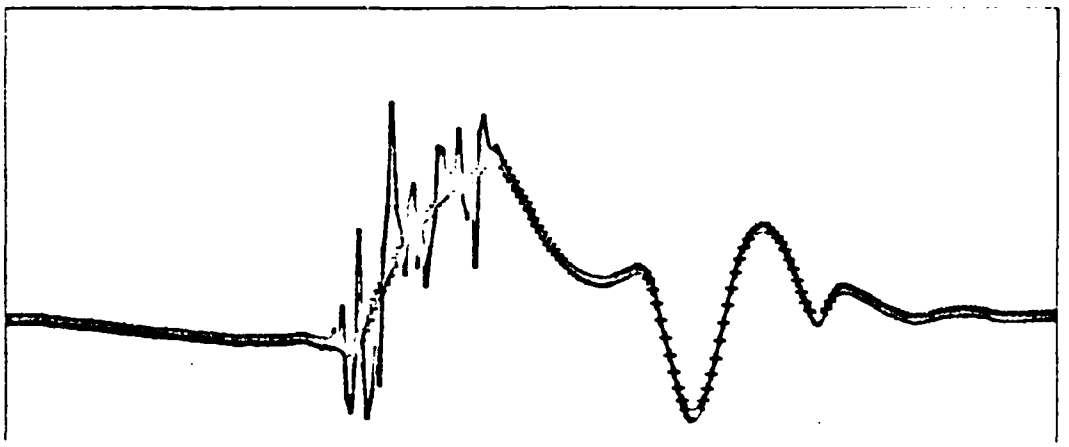

(b)

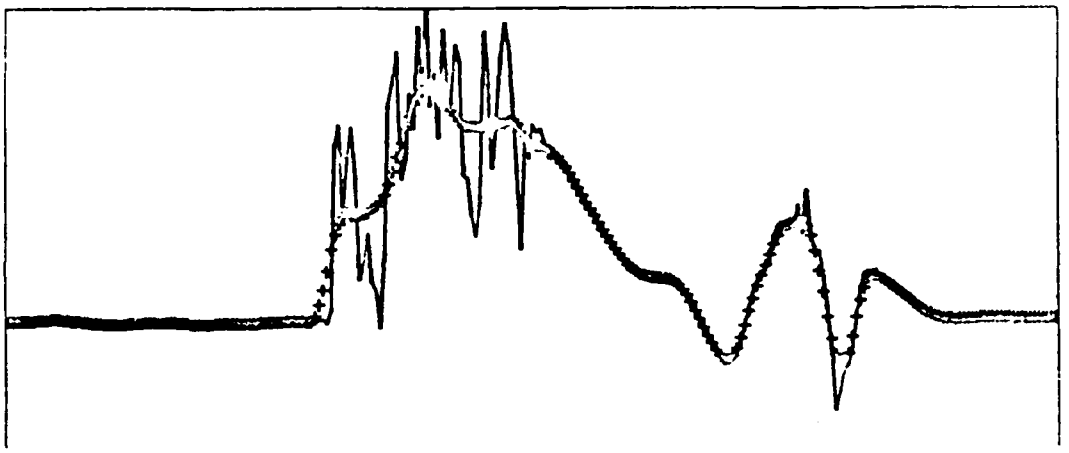

(c)

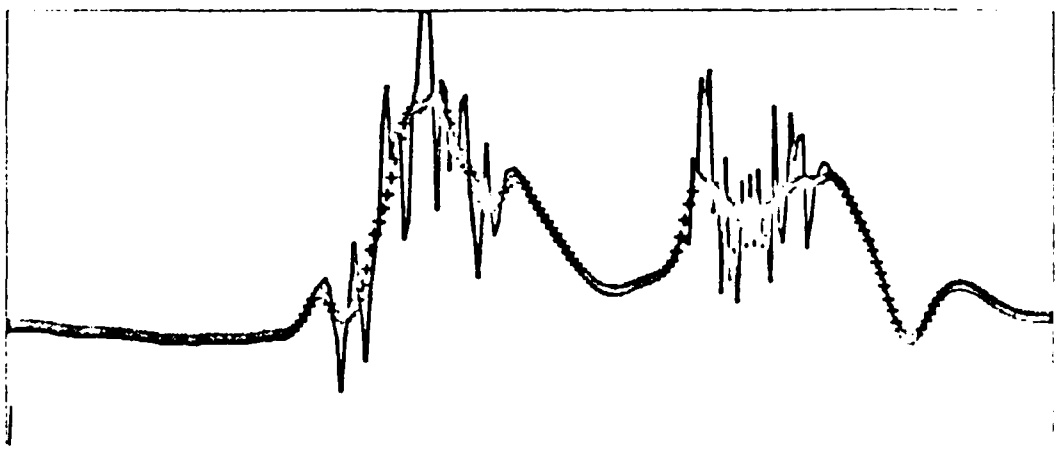

fig 4

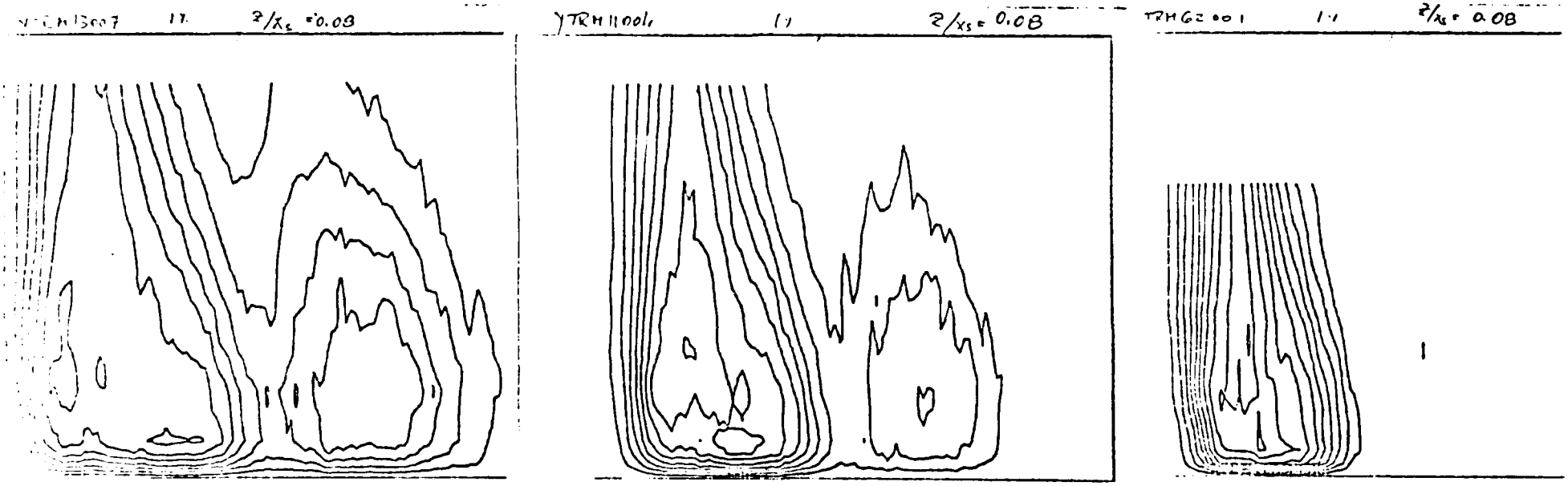

X_S = 1000 mm X_S = 810 mm X_S = 620 mm

fig 6

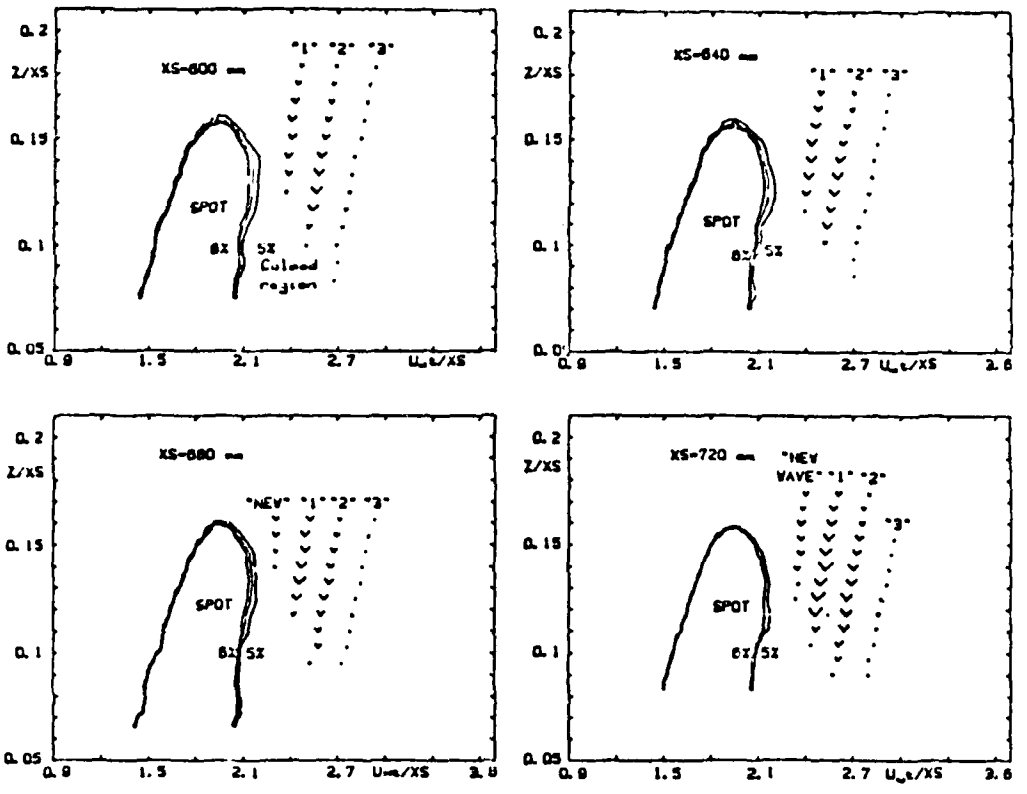
XS=600 mm
XS=640 mm
XS=680 mm
XS=720 mm
SPOT
"NEW" WAVE
"1"
"2"
"3"
δx
δz
Z/XS
0.2
0.15
0.1
0.05
0.9
1.5
2.1
2.7
3.3
3.6
3.8

fig 9

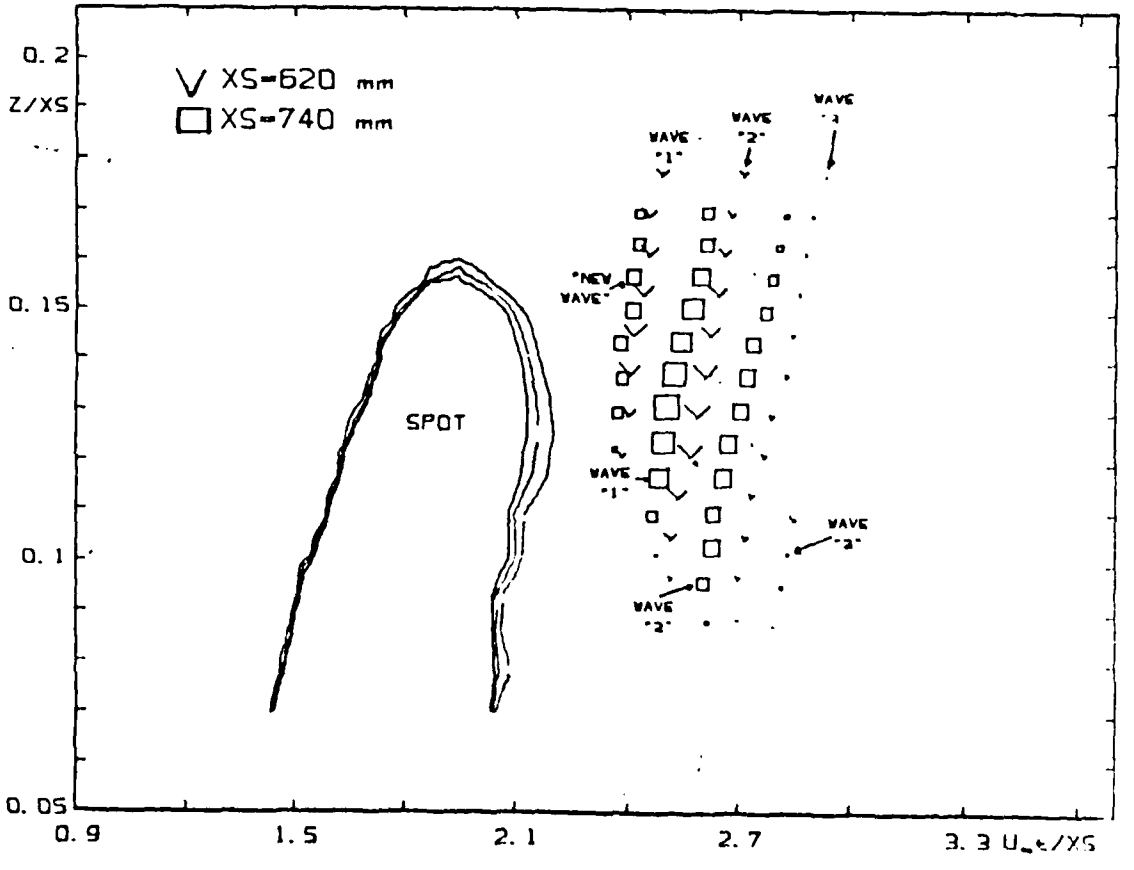
XS=620 mm
XS=740 mm
Z/XS
0.2
0.15
0.1
0.05
SPOT
"NEW" WAVE
"1"
"2"
"3"
0.9
1.5
2.1
2.7
3.3

fig 10

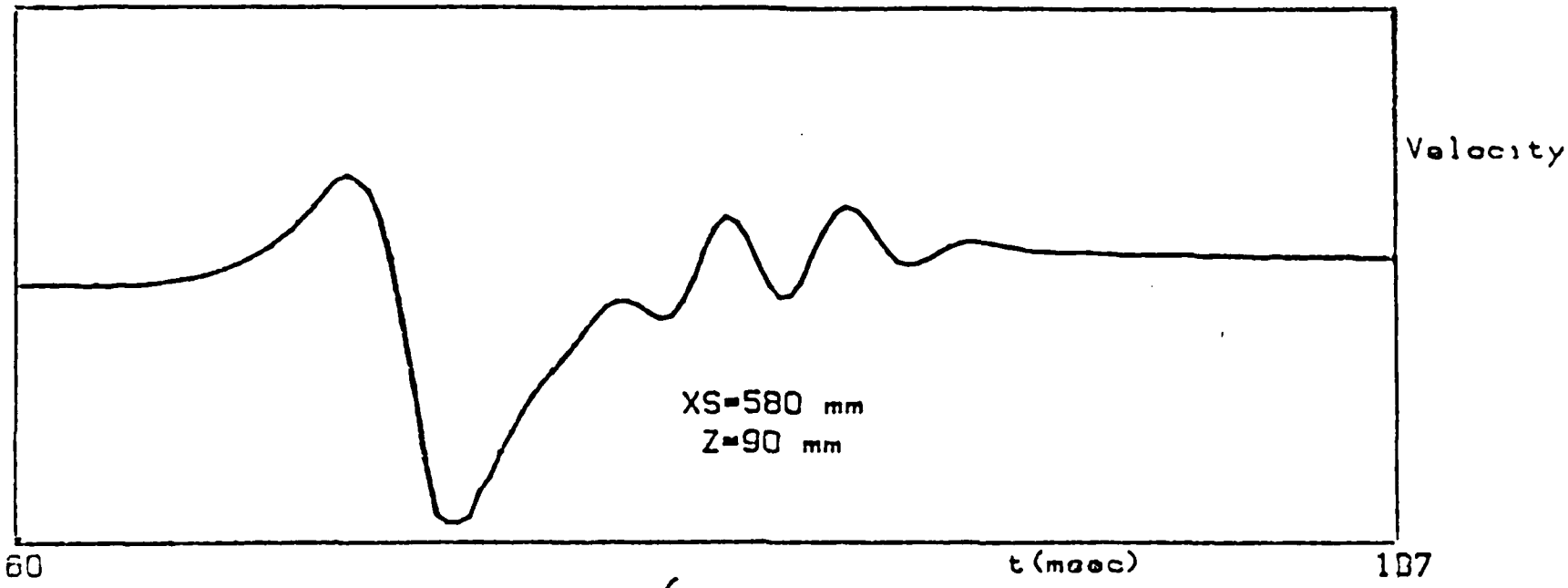
Velocity
XS=580 mm
Z=90 mm
60
t (msec)
107

fig 8

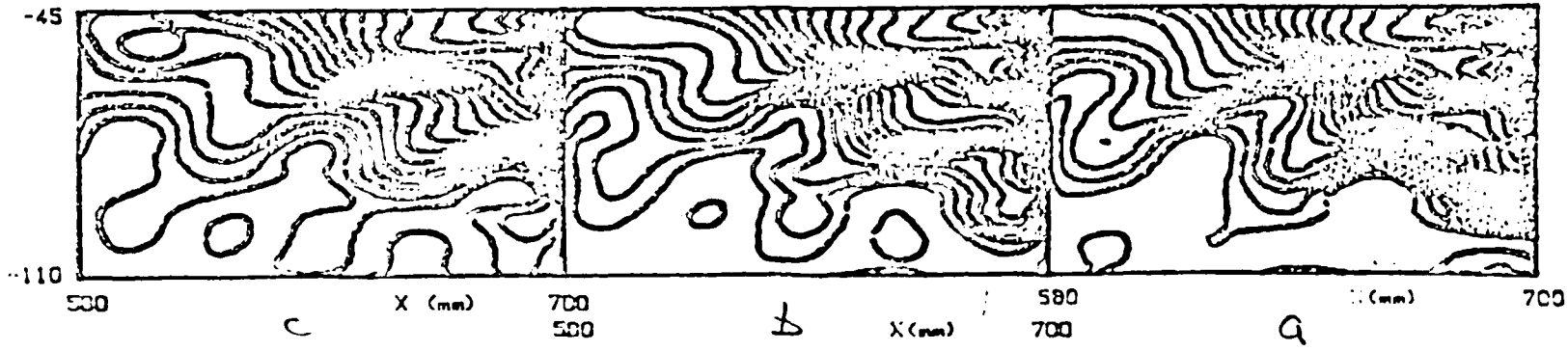
-45
-110
500
X (mm)
700
500
580
700
700

fig 12

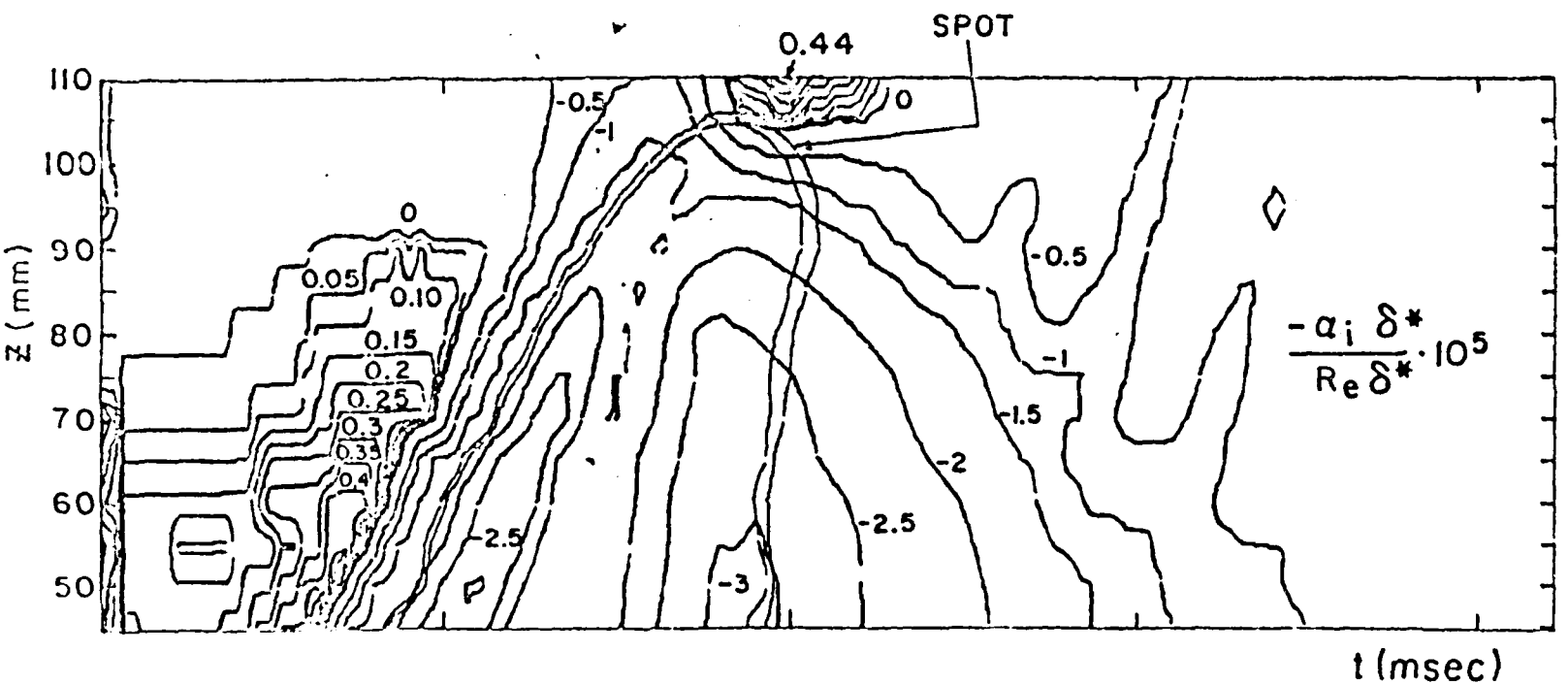

fig 11 CONTOURS OF Imag. Alpha

END

5-87

DTIC